JOURNAL OF Applied Polymer SCIENCE

Permeability and Transport Model of Epoxy Membranes with Various Surface Morphologies

Yu-Shun Luo, Kuo-Chung Cheng, Chiu-Ya Wang, Yi-Min Chang, Ying-Hong Wu, Yi-Ping Chen
Department of Chemical Engineering and Biotechnology, National Taipei University of Technology, Taipei 106, Taiwan
Correspondence to: K.-C. Cheng (E-mail: gordon@ntut.edu.tw)

ABSTRACT: Epoxy membranes that have interconnected pores with different surface structures were synthesized using the chemically induced phase separation process. The epoxy membrane was produced from a mixture of epoxy resin, D.E.R. 331, and the curing agent, 2,4,6-tris-(dimethylaminomethyl) phenol (DMP-30) in diisobutyl ketone, while covered with a contacting film. It was found that the surface morphology of the epoxy membranes could be changed by the fraction of DIBK, or by using different contacting films of which the surface pore sizes ranged from 0.15 through 2.4 μm. Furthermore, ethanol permeabilities through the epoxy membranes were measured. The permeabilities are approximately 3–4700 L/m^2 h bar and depend on either the bulk morphology or the skin structure of the membranes. The epoxy membranes with various porosities and ethanol permeabilities could be also prepared using different compositions of the DMP-30 and diethylene triamine (DETA)) mixture. A modified Hagen–Poiseuille equation was proposed to describe the effects of the surface and bulk porosity on ethanol permeability. It was found that at low permeabilities, most of the resistance of the surface layers is higher than that of the bulk section. © 2013 Wiley Periodicals, Inc. J. Appl. Polym. Sci. 000: 000–000, 2013

KEYWORDS: morphology; membranes; porous materials; separation techniques

Received 2 February 2012; accepted 4 May 2013; Published online
DOI: 10.1002/app.39510

INTRODUCTION

Porous polymers have many useful applications, including use as separation media, foams, chromatography supports, and membranes for cell cultures.[1–5] Many methods have been developed to produce porous polymers with different morphologies. One of these techniques is chemically induced phase separation (CIPS), which is a process where a homogeneous solution of monomers or pre-polymers and solvent become phase separated during polymerization. The porous polymers are then obtained after evaporating the solvent in the matrix by heating or vacuum.[6–12] For example, macroporous epoxy networks with a narrow pore size distribution and closed-cell morphology have been prepared from curing an epoxy resin with a primary amine in the presence of solvent. It has been proposed that the solvent-rich closed domains were formed via nucleation and growth, whereby the pore size and distribution could be controlled by the fraction of solvent. However, it has been reported that when phase separation is induced via step-wise polymerization, it is difficult to obtain bi-continuous structures from the addition of a low-molecular-weight compound, such as a solvent. When an epoxy resin is cured with a primary amine, the polymers mainly grow via step-wise polymerization, which causes a closed-pore structure in the epoxy matrix. Epoxy membranes have several advantages over thermoplastic polymers, such as good chemical resistance and high thermal stability. Therefore, some limits on the application of porous thermoplastic polymers in harsh environments, such as high temperature and low or high pH, could be expected to be overcome using epoxy membranes.[13–15]

In our previous work, it was reported that epoxy membranes with interconnected pores could be prepared by curing a commercial epoxy resin, D.E.R. 331, with a tertiary amine, 2,4,6-tris-(dimethylaminomethyl) phenol (DMP-30), in the presence of a solvent, diisobutyl ketone (DIBK).[16] The permeabilites of different solvents through the prepared epoxy membranes were measured under constant pressure. It was found that the epoxy membranes had high permeability for cyclohexane or ethanol and low permeability for water. However, the permeability and selectivity of polymer membranes depend not only on the bulk structure but also on the surface morphology.[17–20] There are many techniques for controlling the surface morphology of a membrane, such as surface treatment, surface grafting polymerization, templating, or self-assembly methods, which have been applied to produce specific surface structures on polymer films.[21–26] We also demonstrated a novel, simple method for producing porous cross-linked polymers that have similar bulk morphologies and a variety of surface structures through the use of a CIPS process.[27] The surface morphology could be

changed with the use of contacting films with different wetting properties, which were pressed onto the casting solution during curing.

In this study, epoxy membranes were prepared from epoxy resin that was cured with DMP-30 in DIBK that was covered with various contacting films; then, epoxy membranes that have a similar interconnected pore structure with different surface morphologies could be obtained. The dependence of the ethanol permeability on the epoxy membrane structure was further discussed. Finally, a modified Hagen–Poiseuille (H–P) equation was proposed to verify the contribution of the skin or bulk resistance of the epoxy membrane to the ethanol permeability.

EXPERIMENTAL

Materials

Bisphenol A diglycidyl ether epoxy resin (D.E.R. 331, epoxy equivalent weight = 186) was purchased from Dow Chemical Company; the curing agent 2,4,6-tris-(dimethylaminomethyl) phenol (DMP-30, Aldrich), diethylene triamine (DETA, 98%; Panreac), and diisobutyl ketone (DIBK, Acros) were used without further purification. The mixtures were transferred into a mold and covered with various contacting films: silicone-coated oriented polypropylene, OPP (PP3Q, Symbio), Teflon-1 (Polyfluoroalkoxy, PFA), and Teflon-2 (ASF-110, CHUKOH FLO® adhesive tapes, Japan).

Preparation of the Epoxy Membrane

The epoxy resin D.E.R. 331 was mixed with the solvent DIBK in different ratios and stirred to form a homogeneous solution; then the curing agent at 10 phr of DMP-30 or a mixture of DETA and DMP-30 was added into the solution. The solution was transferred into a plate mold and covered and sealed with contacting films that were coated with silicon or Teflon. The solution was cured at approximately 40°C for 24 h. The gelled sample was removed from the mold then placed into a vacuum oven at 170°C for 24 h to post-cure and remove the solvent DIBK.

Characterization of the Membrane Morphology

The cured epoxy membranes that were prepared with various initial compositions were studied using a scanning electron microscope (SEM, Hitachi S-3000H). The surface morphology of the membrane was directly observed by sputtering gold onto the sample, and some specimens were fractured in liquid nitrogen for cross-sectional examination using the SEM.

Measurement of Ethanol Permeability

The cured membrane, with a thickness of approximately 0.25 mm, was mounted between two steel circular rings that had an inner diameter of 13 mm. The flow of ethanol through the membrane was measured at room temperature under 0.8 bar of constant pressure. The permeability J' was calculated using the following equation:

$$J' = \frac{Q}{A \cdot \Delta P}, \tag{1}$$

where Q is the volumetric flow rate of ethanol (99%), A is the cross-sectional area of the membrane, and ΔP is the drop in pressure.

Determination of Membrane Porosity

The membranes were immersed in ethanol to determine their porosities. The weight differences between the dry and wet membrane samples (before and after immersion) were measured, and the membrane porosities could then be determined from the following equation[28,29]:

$$\varepsilon = \frac{W_w - W_d}{\rho_e \times V}, \tag{2}$$

where W_w is the weight of the ethanol wetted membranes, W_d is the weight of the dry membranes, ρ_e is the density of ethanol at room temperature, and V is the volume of the fully wetted membrane.

RESULTS AND DISCUSSION

Morphologies of the Epoxy Membranes

Figure 1 shows the SEM images of the cross-sectional morphologies of the cured epoxy membranes prepared with various fractions of solvent, DIBK, and different contacting films. A dense morphology was formed from the solution with 28 vol % of solvent, sample M-28. A porous structure apparently appeared when the solvent was increased to 32 vol %. Additionally, increasing the fraction of solvent leads to an increase in the samples pore size, and similar tendencies were also found when using different contacting films.

The surface morphology of the epoxy membranes prepared with various fractions of solvent and different contacting films are illustrated in Figure 2. It was found that a dense structure was formed when using 28 vol % of DIBK; however, when the amount of DIBK was greater than approximately 32 vol %, some pores appeared on the surface. Furthermore, the pore diameters were measured from the SEM photograph, and the mean pore diameter was calculated as follows[29]:

$$d_m = \sqrt{\frac{\sum n_i d_i^2}{\sum n_i}} \tag{3}$$

where n_i is the number of pores with diameter d_i. The surface porosity was calculated by taking the sum of all the pore areas in a SEM image then dividing by the total area of the image. As indicated from the SEM images and Table I, the channel diameter and the surface pore size increase with increasing amounts of DIBK. On the surface of the membrane formed under the silicone silicone-coated oriented polypropylene (OPP) contacting film, the pore size was approximately 0.16 μm at 32 vol % of DIBK, and it became 1.44 μm at 40 vol %. The surface porosity also increased from 0.07 to 0.45 when increasing the amount of solvent.

Additionally, when Teflon 1 (PFA) and Teflon 2 were used as the contacting films, the surface pore size and porosity of the membranes formed at high content of DIBK, such as M-38 and M-40, were larger than those formed under silicone (OPP), as indicted in Figure 2 and Table I. At 40% of DIBK, the surface pore size of the membranes prepared under the Teflon 1 and Teflon 2 contacting films are approximately 2.42 and 2.33 μm, respectively. The surface porosities are approximately 0.57 and 0.59 μm. However, under the silicone (OPP) contacting film, the surface pore size and porosity of the membranes are approximately 1.44 and 0.45 μm, respectively. The difference of interfacial tension of the solid/solvent-rich phase and solid/

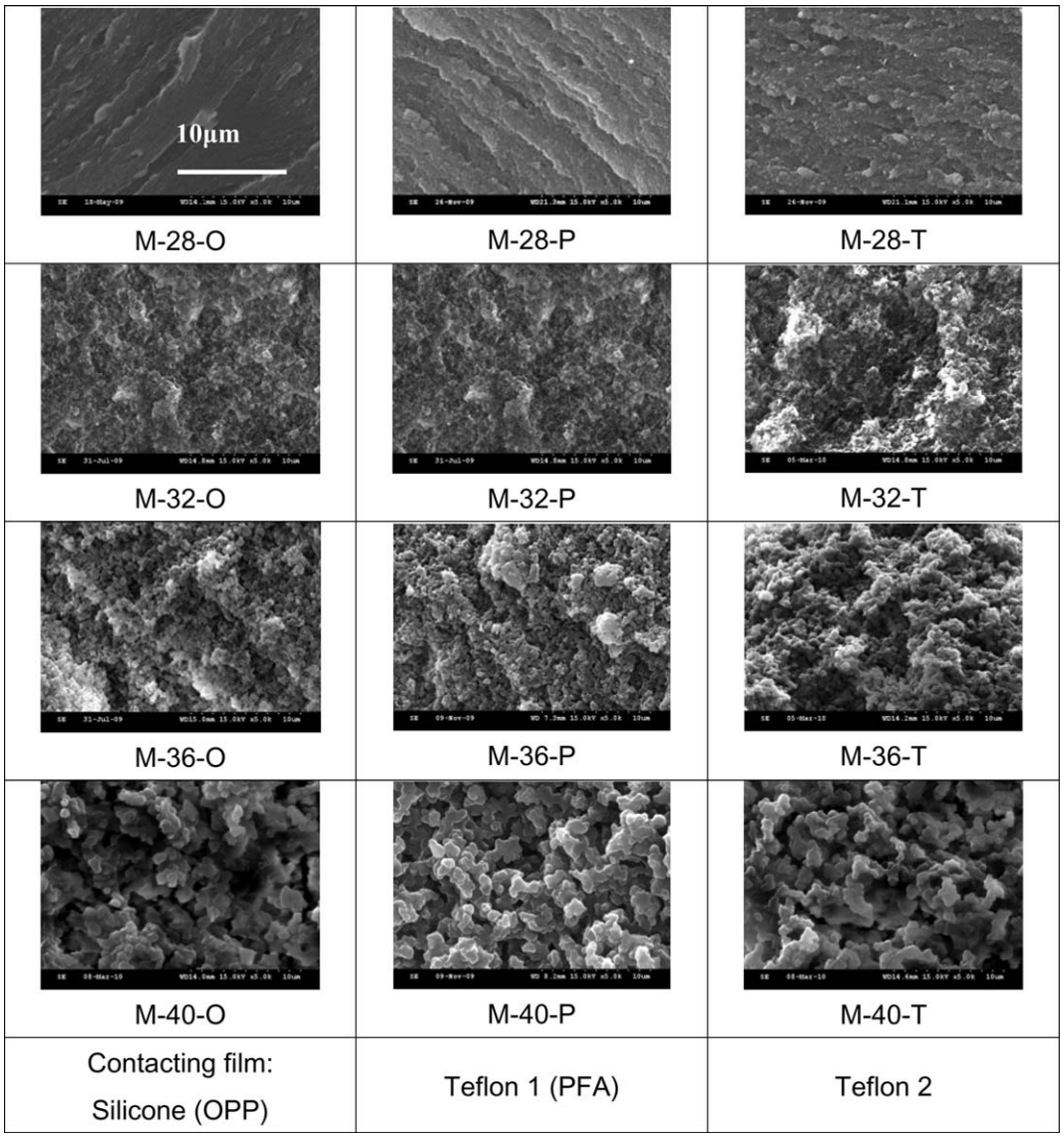

Figure 1. SEM images of the cross-sectional morphologies of the epoxy membranes prepared with various fractions of the solvent (28–40 vol %) under different contacting films.

polymer-rich phase could significantly influence the phase separation process among the interfaces of solid and liquid solutions, and it will cause the different surface morphologies.[27] Therefore, it was suggested that different surface morphologies of epoxy membranes with similar bulk structures can be prepared using CIPS with different contacting films.

Ethanol Permeation Test

The ethanol permeability through the prepared epoxy membrane was measured to investigate the effect of the membrane structure on the permeation behavior, and the results are shown in Figure 3 and Table II. No ethanol flux was detected through the epoxy membrane prepared with 28 vol % of DIBK because of its dense structure. Once the porous morphology was formed, the ethanol could flow through the epoxy membrane. For example, sample M-32-O had lower overall and surface porosities, 0.35 and 0.07, respectively, which resulted in a lower ethanol permeability, J', of approximately 3 L/m^2 h bar. The permeability was increased to 548 L/m^2 h bar because of the higher porosities of the M-38-O sample.

It was also found that the permeability is not only controlled by the bulk porosity but also depends on the surface skin morphology of the epoxy membrane. For instance, the overall porosities of the M-38 sample series were similar, approximately 0.50–0.54, but the surface porosities were very different, from 0.35 to 0.48, which resulted from curing under various contacting films. As indicted in Table II, the ethanol permeability increased with increasing surface porosities. This result implies that the skin flow resistance played an important role in the ethanol permeability of the epoxy membrane.

Epoxy Membrane Prepared by Curing Agent DMP-30/DETA Mixture

Porous epoxy networks can also be prepared by curing an epoxy resin with a primary amine, such as DETA, in DIBK solvent.

Applied Polymer SCIENCE

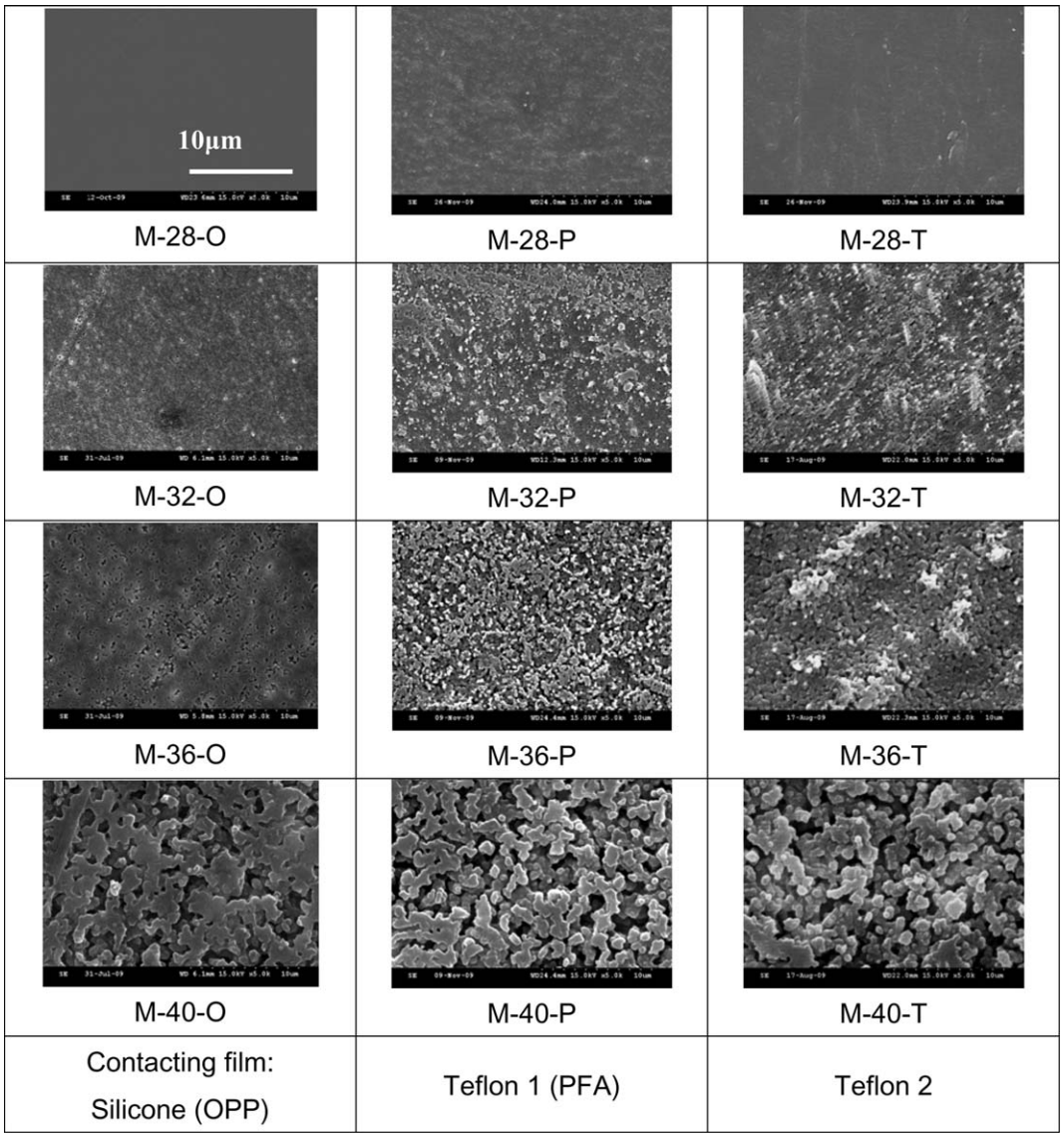

Figure 2. SEM images of the surface morphologies of the epoxy membranes prepared with various fractions of the solvent (28–40 vol %) under different contacting films.

However, most of the porous epoxy network exhibited a closed-pore morphology, which was quite different from those prepared with DMP-30. The different phase separation processes between them had been discussed in the previous study.[16] For the DETA system, the viscosity of the reaction solution increased gradually with the growth of molecular weight of the

Table I. Pore Characteristics of the Epoxy Membranes Formed Under Various Contacting Films

	Surface pore size (μm)			Surface porosity			Cross-section pore size (μm)			Overall porosity		
Sample	O[a]	P	T	O	P	T	O	P	T	O	P	T
M-30	0.15	0.12	0.18	0.05	0.08	0.02	Dense	0.18	Dense	0.26	0.38	0.33
M-32	0.16	0.18	0.20	0.07	0.20	0.07	0.29	0.18	0.64	0.35	0.41	0.41
M-34	0.34	0.31	0.25	0.19	0.21	0.12	0.40	0.28	0.66	0.39	0.40	0.48
M-36	0.47	0.43	0.74	0.24	0.36	0.29	0.41	0.41	0.87	0.48	0.45	0.54
M-38	1.08	1.46	1.10	0.35	0.48	0.43	0.78	2.29	1.03	0.51	0.54	0.50
M-40	1.44	2.42	2.33	0.45	0.57	0.59	1.65	2.23	1.58	0.51	0.51	0.63

[a] Contacting films: O, P, and T denote silicone-coated oriented polypropylene (OPP), Teflon-1 (PFA), and Teflon-2 (ASF-110), respectively.

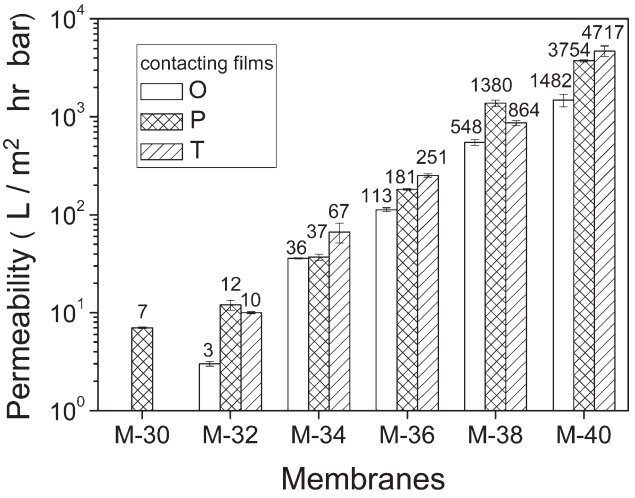

Figure 3. Ethanol permeabilities of the epoxy membranes.

polymers via step-wise polymerization. The separated solvent-rich domains have long time to grow and coarsen as larger isolated cells under low viscosity. On the other hand, for the DMP-30 system, it was found that two-stage phase separation resulted from a complicated polymerization occurred. After the first-stage phase separation, the viscosity of solution increased rapidly. Because the second-phase separation process took place under high viscosity, the slower domain growing rate could help to retain the nascent structure formed by phase separation. The morphology dependent on the composition of the mixture of DMP-30 and DETA is worthy of being further studied.

Figures 4 and 5 show the SEM images of the cross-sectional and surface morphologies, respectively, of the cured epoxy membranes synthesized using various weight ratios of DMP-30/DETA (Table III). With a higher content of DETA as shown in Figure 4(f–i), the polymerization and phase separation mechanisms were dominated by the DETA, which caused a closed-pore structure in the cured epoxy network. Therefore, the ethanol could not flow through these membranes. On the contrary, an interconnected porous morphology could be formed with a higher ratio of DMP-30/DETA. For the samples A3 and 1, the overall porosity increased from 0.4 to 0.49 with increasing amounts of DMP-30, and the ethanol permeability increased from 15 to 64 L/m^2 h bar. Therefore, porous epoxy membranes with various porosities and ethanol permeabilities could be prepared using different compositions of the DMP-30 and DETA mixture.

Modified H–P Equation

To understand the effects of the surface and bulk morphologies of epoxy membranes on permeation behavior, a modified H–P model was proposed to verify the contribution of the skin or bulk flow resistance. The H–P equation describes the relationship between the fluid velocity and the pressure drop through a capillary. Provided the membrane is regarded as a bundle of capillaries with tortuosity (τ), and length (L), the dependence of the permeability on the membrane structure can be described as follows:

$$J = \frac{\Delta P \cdot d_m^2 \cdot \varepsilon}{32\mu \cdot L \cdot \tau} \quad (4)$$

where J is the flux, ΔP is the pressure drop between the two ends of the channel, d_m is the pore diameter, ε is the porosity,

Table II. Ethanol Flux and Resistances of the Epoxy Membranes

Contacting films	Sample	R_1 ($\times 10^{-11}$ m^{-1})	R_2 ($\times 10^{-11}$ m^{-1})	$R_1 + R_2$ ($\times 10^{-11}$ m^{-1})	J',(a) (L/m^2 h bar)	J'exp,(b) (L/m^2 h bar)	Thickness of membrane (mm)
Silicone (OPP)	M-32-O	797.2	75.6	872.8	3	3	0.25
	M-34-O	23.9	32.7	56.6	53	36	0.24
	M-36-O	7.9	21.1	29.0	103	113	0.25
	M-38-O	0.7	5.1	5.8	519	548	0.25
	M-40-O	0.2	1.1	1.3	2192	1482	0.25
Teflon 1 (PFA)	M-30-P	1085.1	173.2	1258.3	2	7	0.22
	M-32-P	77.2	144.1	221.3	14	12	0.25
	M-34-P	23.6	62.5	86.1	35	37	0.26
	M-36-P	4.2	23.6	27.8	108	181	0.25
	M-38-P	0.2	0.5	0.7	4136	1380	0.27
	M-40-P	0.1	0.6	0.7	4501	3754	0.25
Teflon 2	M-32-T	510.2	11.5	521.7	6	10	0.26
	M-34-T	111.1	7.9	119.0	25	67	0.26
	M-36-T	2.2	3.6	5.8	518	251	0.28
	M-38-T	0.5	3.0	3.5	866	864	0.27
	M-40-T	0.1	0.9	1.0	3188	4717	0.25
Silicone (OPP)	A-1	4.6	10.6	15.2	197	64	0.23
	A-2	39.4	20.2	59.6	50	33	0.23
	A-3	206.6	24.7	231.3	13	15	0.24

[a] Calculated results [eq. (10)], [b] Experimental data.

Applied Polymer SCIENCE

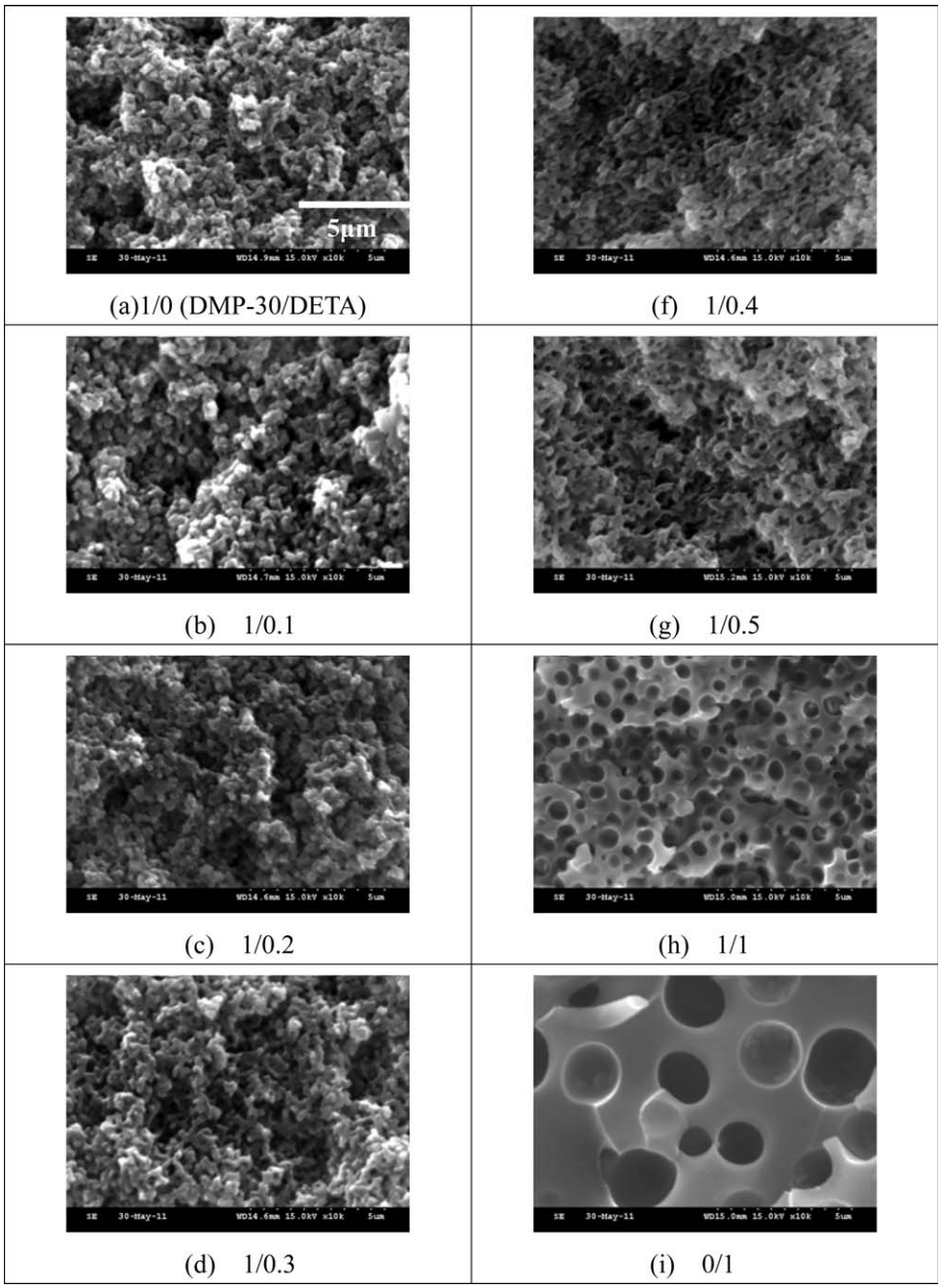

Figure 4. SEM images of the cross-sectional morphologies of the epoxy membranes cured with DMP-30/DETA.

and μ is the viscosity of fluid. The tortuosity of the capillary can be regarded as the reciprocal of ε[28,30]; therefore, eq. (4) becomes

$$J = \frac{\Delta P \cdot d_m^2 \cdot \varepsilon^2}{32k \cdot \mu \cdot L}, \quad (5)$$

where k is assumed to be a constant in this study. Furthermore, the flux can be expressed by Darcy's law[26]:

$$J = \frac{\Delta P}{\mu \cdot R}, \quad (6)$$

where R denotes the flow resistance of a fluid through a porous medium, and it can be calculated by eq. (7):

$$R = \frac{32k \cdot L}{(d_m^2 \cdot \varepsilon^2)} \quad (7)$$

As observed in the SEM images, the surface morphology of the prepared epoxy membrane might not be similar to the bulk section. This observation suggests that the flow resistances of the surface skin and bulk section could be different. Therefore, we introduced R_1 to represent the flow resistance of the top and bottom skin layers and R_2 as the resistance of the bulk section.

$$R_1 = \frac{K_1}{(d_{m1}^2 \cdot \varepsilon_1^2)} \quad (8)$$

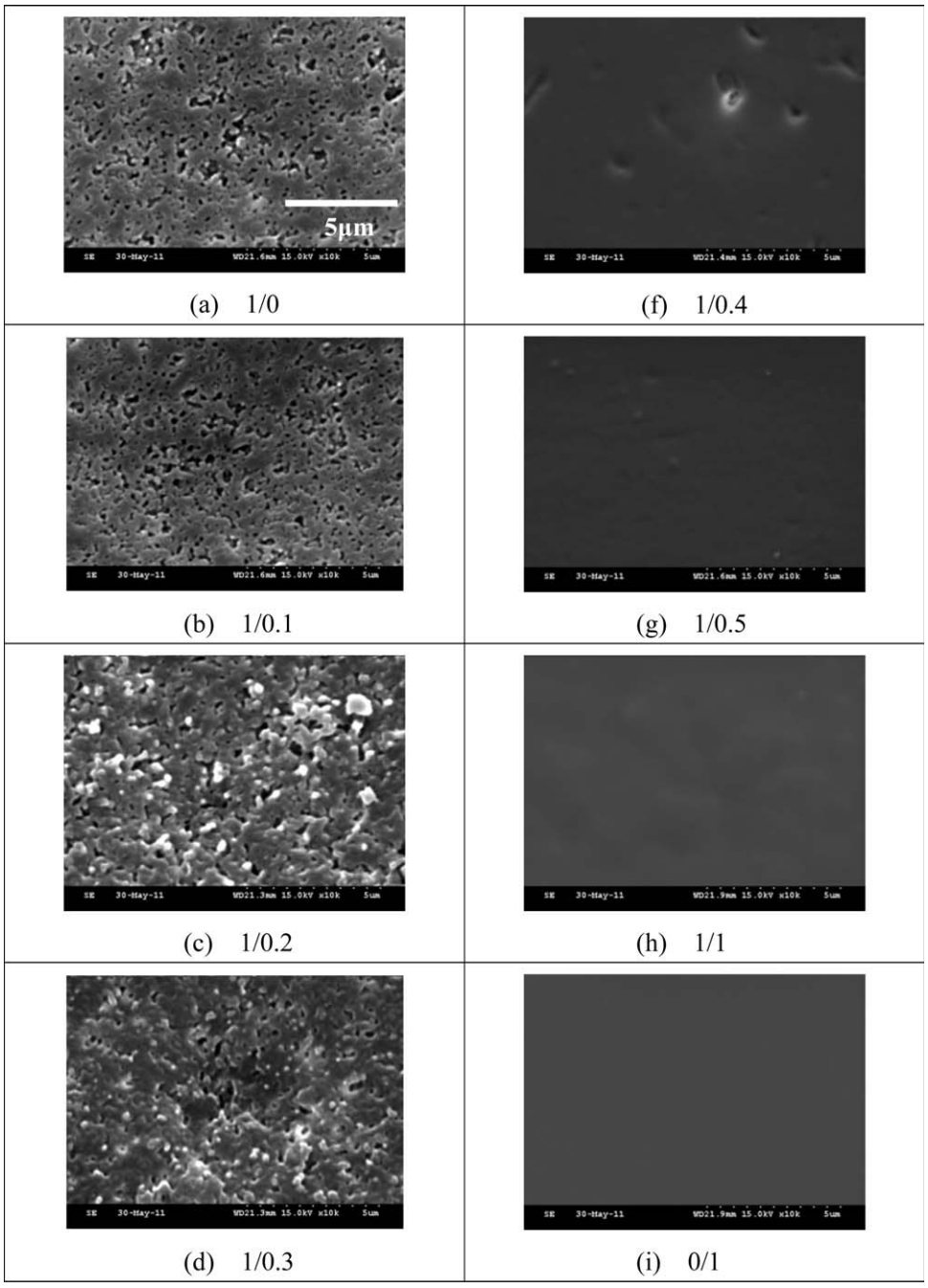

Figure 5. SEM images of the surface morphologies of the epoxy membranes cured with DMP-30/DETA.

Table III. Pore Structures and Ethanol Permeabilities of the Epoxy Membranes Prepared Using D.E.R. 331 Cured with DMP-30/DETA in 34 vol % of DIBK with silicon coated OPP contacting films

Sample	DMP-30/DETA (w/w)	Surface pore size (μm)	Surface porosity	Cross-section pore size (μm)	Overall porosity	J' (L/m^2 h bar)
M-34-0	1/0	0.34	0.19	0.40	0.39	36
A-1	1/0.1	0.36	0.41	0.56	0.49	64
A-2	1/0.2	0.28	0.18	0.51	0.39	33
A-3	1/0.3	0.22	0.10	0.45	0.40	15
A-4	1/0.4	Closed-pore				0

$$R_2 = \frac{K_2}{(d_{m2}^2 \cdot \varepsilon_2^2)} \quad (9)$$

where $K_1 = 32\ k_1 \times L_1$; and $K_2 = 32\ k_2 \times L_2$. The L_1 and L_2 parameters denote the thicknesses of the surface skins and the bulk section of the membrane, respectively, and k_1 and k_2 are assumed as constants. The overall membrane flow resistance, R, is assumed as the summation of R_1 and R_2[31]; then eq. ((5)) can be modified as

$$J'\mu = \frac{J \cdot \mu}{\Delta P} = \frac{1}{R} = \frac{1}{(R_1 + R_2)} = \frac{1}{K_1 \cdot \frac{1}{(\varepsilon_1^2 \cdot d_{m1}^2)} + K_2 \cdot \frac{1}{(\varepsilon_2^2 \cdot d_{m2}^2)}} \quad (10)$$

The K_1 and K_2 parameters can be calculated from a non-linear regression analysis of the experimental data in Tables (I–III). It was found that K_1 and K_2 are approximately 0.009 and 0.095 m, respectively. The comparison of the model and experimental J' versus the total resistance, which is the summation of R_1 and R_2, is plotted in Figure 6. According to the modified H–P model, eq. ((10)), the calculated results are in good agreement with the experimental data. The contribution of the resistance of the skin layer, R_1, related to the ethanol permeability J' is plotted in Figure 7. At low permeabilites, less than approximately 20 L/m^2 h bar, most of the fraction of R_1 is larger than 0.5. This result implies that the low value of J' was primarily caused by the skin resistance.

CONCLUSIONS

Epoxy membranes that have a similar interconnected pore bulk structure with various surface morphologies have been successfully prepared from the epoxy resin D. E. R. 331 that was cured with DMP-30 in DIBK and covered with various contacting films. The surface pore size of the epoxy membrane depends not only on the initial composition of the curing solution but also on the contacting film with different wetting properties for the reacting compounds and solvent. It was found that ethanol permeability is not only controlled by the bulk porosity but also depends on the surface skin morphology of the epoxy membrane. A modified H–P equation was proposed to describe the relationship between the permeability J' and the flow resistances of the skin layers and the bulk section, R_1 and R_2, of the epoxy membrane. According to the calculation, the low ethanol permeability primarily resulted from the skin resistance R_1. In other words, the reduced skin flow resistance could drastically increase the ethanol flux through the epoxy membrane.

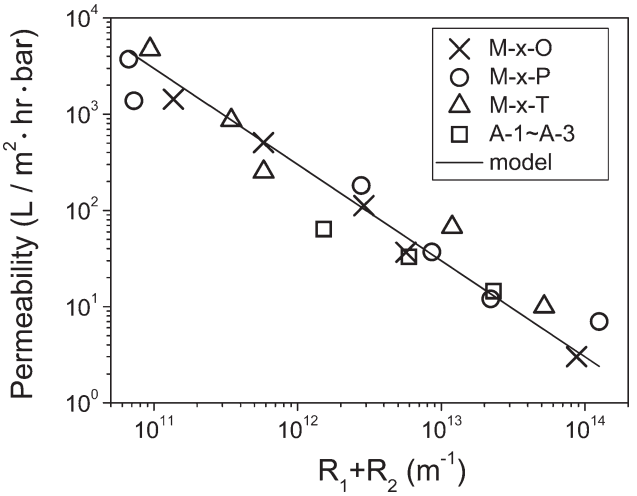

Figure 6. Comparison of the ethanol permeabilities between the experimental data and calculated results according to the modified H–P model.

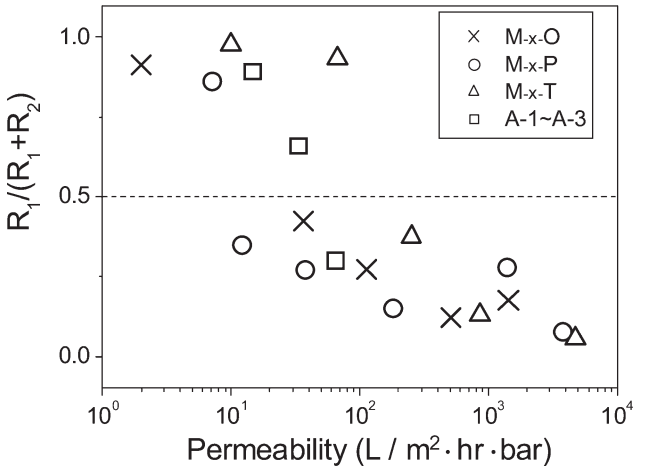

Figure 7. Contribution of the resistance of the skin layer R_1 related to the ethanol permeability J'.

ACKNOWLEDGMENTS

The authors thank the National Science Council of Taiwan for the financial support of this study under Contract NSC 97-2221-E-027-013-MY2.

NOMENCLATURE

A	Cross-sectional area of the membrane
d_1, d_2	Pore sizes of the surface skins and bulk section of the membrane, respectively
d_i	Pore size measured by the SEM image
d_m	Mean pore diameter
J	Flux of ethanol
J'	Permeability
K	Parameter to specify the relationship between tortuosity and porosity
K_1	$= 32k_1 \times L_1$
K_2	$= 32k_2 \times L_2$
L	Thickness of the membrane
L_1, L_2	Thickness of the surface skins and bulk section of the membrane, respectively
n_i	Number of pores with diameter d_i measured from the SEM image
ΔP	Pressure drop
Q	Volumetric flow rate of ethanol through the membrane
R	Overall flow resistance
R_1, R_2	Flow resistances of the surface skins and bulk section of the membrane, respectively.
V	Volume of the fully wetted membrane
W_w	Weight of the ethanol wetted membrane
W_d	Weight of the dry membrane

GREEK LETTERS

ε	Membrane porosity
ε_1, ε_2	Porosity of the surface skins and bulk section of the membrane, respectively
μ	Viscosity
ρ_e	Density of ethanol at room temperature
τ	Tortuosity of the channel

REFERENCES

1. Lewandowski, K.; Svec, F.; Fréchet, J. M. J. *J. Appl. Polym. Sci.* **1998**, *67*, 597.
2. Svec, F.; Fréchet, J. M. J. *Science* **1996**, *273*, 205.
3. Hensema, E. R. *Adv. Mater.* **1994**, *6*, 269.
4. Sotiropoulou, S.; Vamvakaki, V.; Chaniotakis, N. A. *Biosens. Bioelectron.* **2005**, *20*, (8 SPEC. ISS.), 1674.
5. Huck, C. W.; Bonn, G. K. *Chem. Eng. Technol.* **2005**, *28*, 1457.
6. Kiefer, J.; Hilborn, J. G.; Hedrick, J. L. *Polymer* **1996**, *37*, 5715.
7. Kiefer, J.; Hilborn, J. G.; Hedrick, J. L.; Cha, H. J.; Yoon, D. Y.; Hedrick, J. C. *Macromolecules* **1996**, *29*, 8546.
8. Kiefer, J.; Hedrick, J. L.; Hilborn, J. G. *Adv. Polym. Sci.* **1999**, *147*, 163.
9. Garcia Loera, A.; Dumon, M.; Pascault, J. P. *Macromol. Symp.* **2000**, *151*, 341.
10. Ai, H.; Xu, K.; Chen, W.; Liu, H.; Chen, M. *Polym. Int.* **2009**, *58*, 105.
11. Loera, A. G.; Cara, F.; Dumon, M.; Pascault, J. P. *Macromolecules* **2002**, *35*, 6291.
12. Tsujioka, N.; Ishizuka, N.; Tanaka, N.; Kubo, T.; Hosoya, K. *J. Polym. Sci. Part A: Polym. Chem.* **2008**, *46*, 3272.
13. Williams, R. J. J.; Rozenberg, B. A.; Pascault, J. P. *Adv. Polym. Sci.* **1997**, *128*, 95.
14. Jayalakshmi, A.; Rajesh, S.; Senthilkumar, S.; Mohan, D. *Sep. Purif. Technol.* **2012**, *90*, 120.
15. Sforça, M. L.; Yoshida, I. V. P. *J. Membr. Sci.* **1999**, *159*, 197.
16. Luo, Y.-S.; Cheng, K.-C.; Wu, C.-L.; Wang, C.-Y.; Tsai, T.-H.; Wang, D.-M. *Colloid Polym. Sci.*, (Published online: 5 March 2013).
17. Knoell, T.; Safarik, J.; Cormack, T.; Riley, R.; Lin, S. W.; Ridgway, H. *J. Membr. Sci.* **1999**, *157*, 117.
18. Ji, Y.; Li, X. M.; Yin, Y.; Zhang, Y. Y.; Wang, Z. W.; He, T. *J. Membr. Sci.* **2010**, *353*, 159.
19. Stawikowska, J.; Livingston, A.G. *J. Membr. Sci.* **2013**, *425–426*, 58.
20. Shirazi, M. M. A.; Bastani, D.; Kargari, A.; Tabatabaei, M. *Desalination Water Treat.*, (Published online: 11 Feb 2013).
21. Holland, B. T.; Blanford, C. F.; Stein, A. *Science* **1998**, *281*, 538.
22. Walheim, S.; Schäffer, E.; Mlynek, J.; Steiner, U. *Science* **1999**, *283*, 520.
23. Widawski, G.; Rawiso, M.; François, B. *Nature* **1994**, *369*, 387.
24. Monnier, A.; Schuth, F.; Huo, Q.; Kumar, D.; Margolese, D.; Maxwell, R. S.; Stucky, G. D.; Krishnamurty, M.; Petroff, P.; Firouzi, A.; Janicke, M.; Chmelka, B. F. *Science* **1993**, *261*, 1299.
25. Park, M.; Harrison, C.; Chaikin, P. M.; Register, R. A.; Adamson, D. H. *Science* **1997**, *276*, 1401.
26. Li, Z.; Zhao, W.; Liu, Y.; Rafailovich, M. H.; Sokolov, J.; Khougaz, K.; Eisenberg, A.; Lennox, R. B.; Krausch, G. *J. Am. Chem. Soc.* **1996**, *118*, 10892.
27. Luo, Y. S.; Cheng, K. C.; Huang, N. D.; Chiang, W. P.; Li, S. F. *J. Polym. Sci. Part B: Polym. Phys.* **2011**, *49*, 1022.
28. Li, W.; Xing, W.; Xu, N. *Desalination* **2006**, *192*, 340.
29. Chakrabarty, B.; Ghoshal, A. K.; Purkait, M. K. *J. Colloid Interface Sci.* **2008**, *320*, 245.
30. Johnston, P. R. *Filtr. Sep.* **1998**, *35*, 287.
31. Darvishmanesh, S.; Buekenhoudt, A.; Degrève, J.; Van der Bruggen, B. *Sep. Purif. Technol.* **2009**, *70*, 46.